Méthodes de spectroscopie d'émission pour le diagnostic des plasma produits par ablation laser

Jörg Hermann

LP3, CNRS, Aix-Marseille Université, 13009 Marseille

Méthodes de spectroscopie d'émission

pour le diagnostic des plasma produits par ablation laser

Emission from laser-produced plasmas

Spectral line profile

Electron density measurement

Local thermodynamic equilibrium

Temperature measurement

Self-absorption

Non-uniform spatial distribution

Méthodes de spectroscopie d’émission

pour le diagnostic des plasma produits par ablation laser

Emission from laser-produced plasmas

Spectral line profile

Electron density measurement

Local thermodynamic equilibrium

Temperature measurement

Self-absorption

Non-uniform spatial distribution

Emission from laser-produced plasmas

Material ablation with a ns-laser

E_{las} = 10 mJ
d_{spot} = 100 µm
} F_{las} = 100 Jcm^{-2}

⇨ **10^{14} atomes (≅ 10 ng)**

☞ laser heats material to some 10^4 K

☞ plume expansion u ≅ some 10^3 m s^{-1}

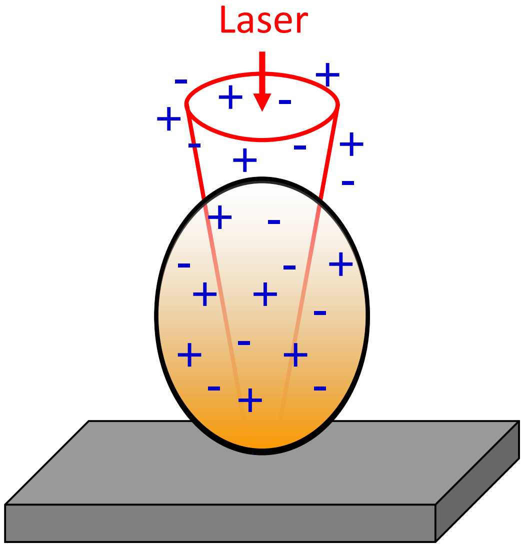

t = 100 ns ⇨ V = 0.1 mm^3

⇨ **plasma density ≅ 10^{18} cm^{-3}** ⇨ **LTE valid**

☞ further plasma evolution depends on surrounding atmosphere

in air, t = 1 µs ⇨ **n_e ≅ 10^{17} cm^{-3}**

⇨ **plasma in LTE for several µs**

Emission from laser-produced plasmas

types of radiation : **intensity**

spontaneous emission

$A^u \Rightarrow A^l + h\nu$ ⇨ **spectral lines** $\propto \quad n_u = n \dfrac{g_u}{Q(T)} e^{-E_u/kT}$

radiative recombination

$A^+ + e^- \Rightarrow A + h\nu$

bremsstrahlung

$A + e^- (E) \Rightarrow A + e^- (E') + h\nu$

} **continuum** $\propto n_e^{\,2}$

plume expansion

⇨ strong decrease of electron density

early expansion stage :

☞ **continuum dominates spectrum**

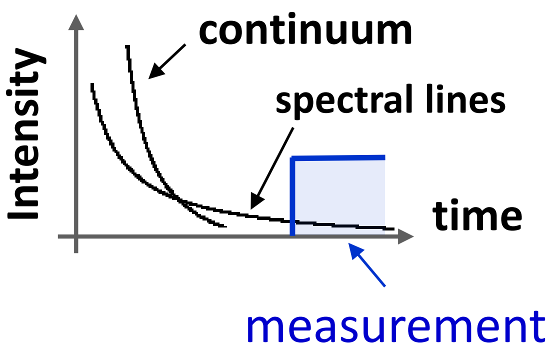

Emission from laser-produced plasmas

Time-evolution of emission spectrum

Titanium, plasma size = 1 mm

T = 6000 K, *n* = 1×10^{16} cm^{-3}

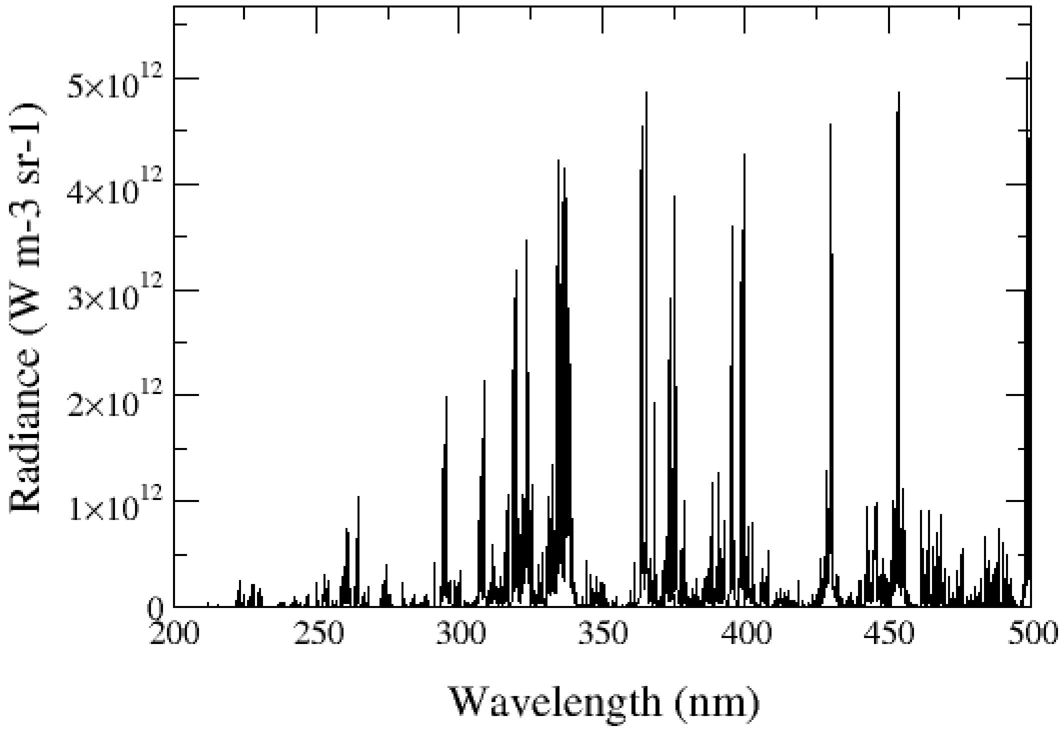

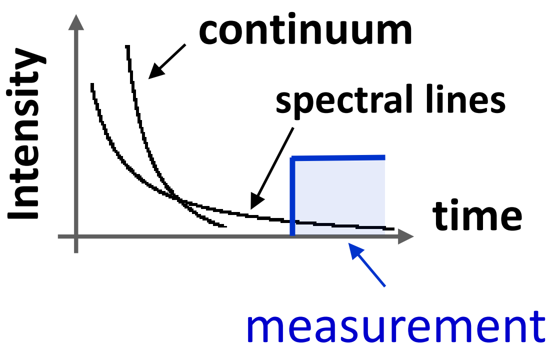

Méthodes de spectroscopie d'émission

pour le diagnostic des plasma produits par ablation laser

Emission from laser-produced plasmas

Spectral line profile

Electron density measurement

Local thermodynamic equilibrium

Temperature measurement

Self-absorption

Non-uniform spatial distribution

Spectral line profile

- Natural broadening

Heisenberg: $\Delta E \, \Delta t \geq h$

example :

$A_{ul} = 10^8$ s^{-1} $\Rightarrow$ $\Delta \nu = 10^8$ s^{-1}

$\Delta \lambda = 0.1$ pm

- Doppler broadening (thermal agitation)

$$\Delta\lambda_{FWHM} = 7.16\times10^{-7}\,\lambda_0\sqrt{\frac{T(K)}{M(amu)}}$$

hydrogen, $T = 10^4$ K $\Rightarrow$ $\Delta\lambda = 50$ pm

- Collisional broadening

impact approximation ☞ collisions interrupt emission process

quasi-static approximation ☞ perturbation of energy levels

type of interaction :

Van der Waals ☞ collisions with neutral particles

Coulomb (Stark effect) ☞ collisions with charged particles

in strongly ionized laser-induced plasmas

☞ **Stark broadening is dominant**

H_α 656 nm, $n_e = 10^{17}$ cm^{-3}

$\Rightarrow$ $\Delta\lambda \cong 1$ nm

Spectral line profile

strongly ionized LIBS plasmas

☞ collisions dominated by electrons

⇨ impact approximation

⇨ linear dependence $\Delta\lambda_{Stark} = w \frac{n_e}{n_e^{ref}}$

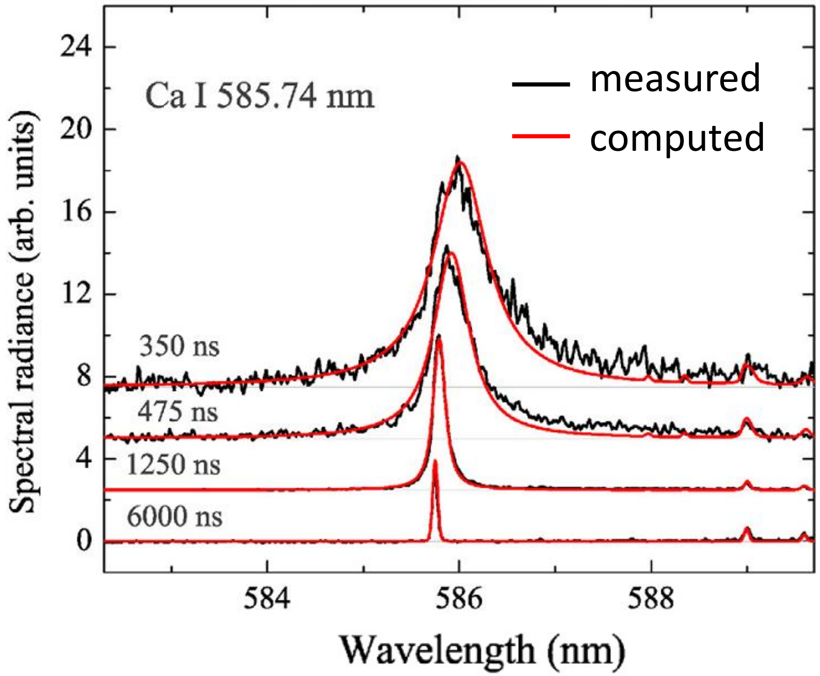

Stark broadening

☞ Lorentz profile

$$L(\lambda,\Gamma) = \frac{2}{\pi\Gamma} \times \frac{1}{1+\left(\frac{\lambda-\lambda_0}{\Gamma/2}\right)^2}$$

Doppler broadening

☞ Gauss profile

$$G(\lambda,\sigma) = \frac{1}{\sigma\sqrt{2\pi}}\, e^{-\frac{1}{2}\left(\frac{\lambda-\lambda_0}{\sigma}\right)^2}$$

depending on relative contributions of Doppler and Stark effects

☞ line shape described by Gauss, Lorentz or Voigt profile

Voigt profile : $V(\lambda,\sigma,\Gamma) = \int_{-\infty}^{+\infty} G(\lambda',\sigma)\, L(\lambda-\lambda',\Gamma)\, d\lambda'$

FWHM =

$\Delta\lambda_L = 2\Gamma$

$\Delta\lambda_G = 2\sigma\sqrt{2\ln(2)}$

Spectral line profile

apparatus broadening

measured line shape ☞ broadening due to spectroscopic apparatus

resolving power of spectrometer $$\frac{\lambda}{\Delta\lambda} = zN$$

z = order of diffraction

N = number of "illuminated" lines of diffraction grating

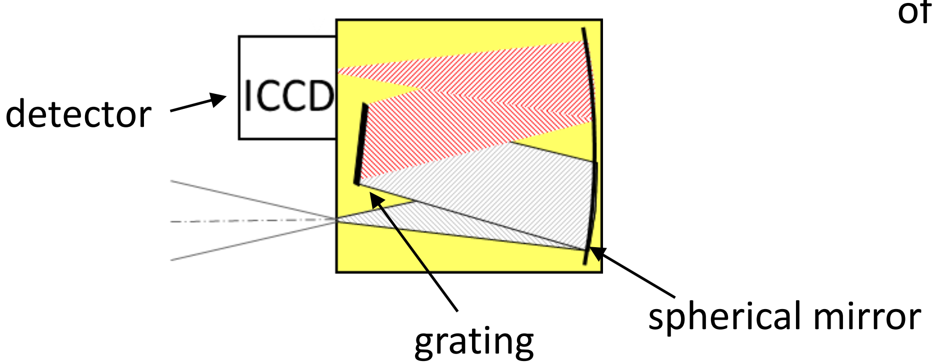

☞ apparatus broadening depends on observation geometry

⇨ $\Delta\lambda_{app} = f(\lambda)$ to be measured with appropriate source

(low pressure (Hg + Ar) discharge lamp)

Spectral line profile

measured line profile

☞ **convolution of computed line shape with apparatus profile**

simplification

☞ apparatus profile ≈ Gauss profile

⇨

$$I_{meas}(\lambda,\Delta\lambda_{app}) = \int_{-\infty}^{+\infty} G(\lambda',\Delta\lambda_{app})\; I_{plasma}(\lambda-\lambda')\, d\lambda'$$

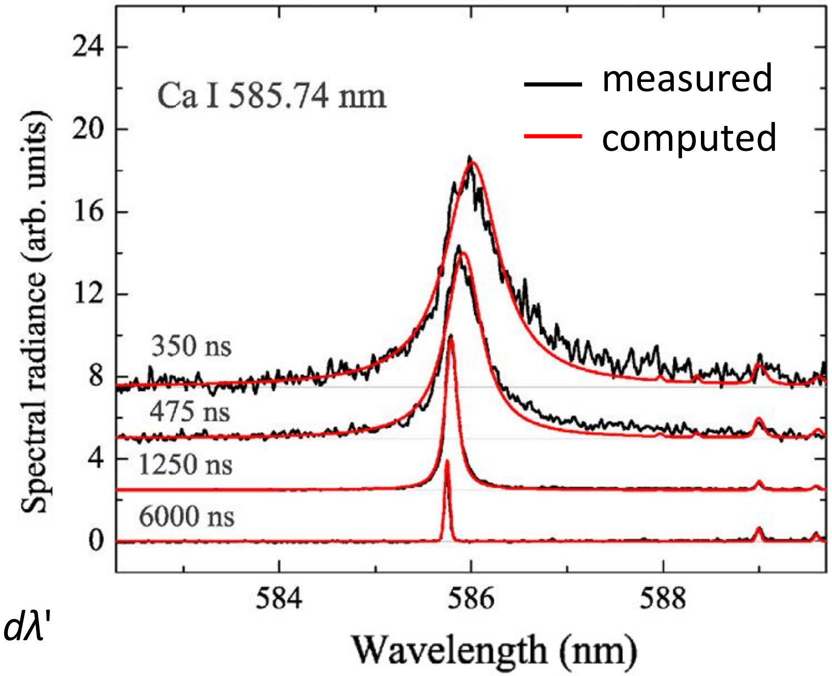

most accurate approach ☞ simulation

alternative solution ☞ line width measurement

relation between FWHM : $\Delta\lambda_V \approx \Delta\lambda_L/2 + \sqrt{\Delta\lambda_L^2/4 + \Delta\lambda_G^2}$

FWHM =

$\Delta\lambda_L = 2\Gamma$

$\Delta\lambda_G = 2\sigma\sqrt{2\ln(2)}$

Méthodes de spectroscopie d'émission

pour le diagnostic des plasma produits par ablation laser

Emission from laser-produced plasmas

Spectral line profile

Electron density measurement

Local thermodynamic equilibrium

Temperature measurement

Self-absorption

Non-uniform spatial distribution

Electron density measurement

using Stark broadening

Stark width $\Delta\lambda_{Stark} = f(n_e, T)$

Table 20. FWHM of Balmer-α (in nm). $\mu = 0.5$.

log(N_e) (m^{-3})	Temperature (K) 5000	10 000	15 000	20 000	30 000	40 000
20.00	1.40 (−2)	1.30 (−2)	1.21 (−2)	1.13 (−2)	9.82 (−3)	8.53 (−3)
20.33	2.41 (−2)	2.34 (−2)	2.23 (−2)	2.13 (−2)	1.93 (−2)	1.75 (−2)
20.67	3.95 (−2)	4.08 (−2)	4.03 (−2)	3.93 (−2)	3.69 (−2)	3.44 (−2)
21.00	6.36 (−2)	6.71 (−2)	6.78 (−2)	6.75 (−2)	6.58 (−2)	6.36 (−2)
21.33	1.01 (−1)	1.09 (−1)	1.12 (−1)	1.13 (−1)	1.13 (−1)	1.12 (−1)
21.67	1.58 (−1)	1.75 (−1)	1.82 (−1)	1.86 (−1)	1.89 (−1)	1.89 (−1)
22.00	2.47 (−1)	2.76 (−1)	2.90 (−1)	2.99 (−1)	3.08 (−1)	3.13 (−1)
22.33	3.89 (−1)	4.35 (−1)	4.60 (−1)	4.76 (−1)	4.95 (−1)	5.06 (−1)
22.67	6.20 (−1)	6.86 (−1)	7.24 (−1)	7.51 (−1)	7.88 (−1)	8.14 (−1)
23.00	1.02 (+0)	1.10 (+0)	1.15 (+0)	1.19 (+0)	1.25 (+0)	1.29 (+0)
23.33	1.68 (+0)	1.79 (+0)	1.86 (+0)	1.91 (+0)	1.99 (+0)	2.05 (+0)
23.67	2.83 (+0)	2.97 (+0)	3.05 (+0)	3.12 (+0)	3.21 (+0)	3.29 (+0)
24.00	—	5.00 (+0)	5.12 (+0)	5.20 (+0)	5.30 (+0)	5.37 (+0)
24.33	—	8.53 (+0)	8.69 (+0)	8.79 (+0)	8.89 (+0)	8.94 (+0)
24.67	—	—	1.47 (+1)	1.50 (+1)	1.52 (+1)	1.53 (+1)

The notation '1.27 (−3)' has been used to represent 1.27×10^{-3}.

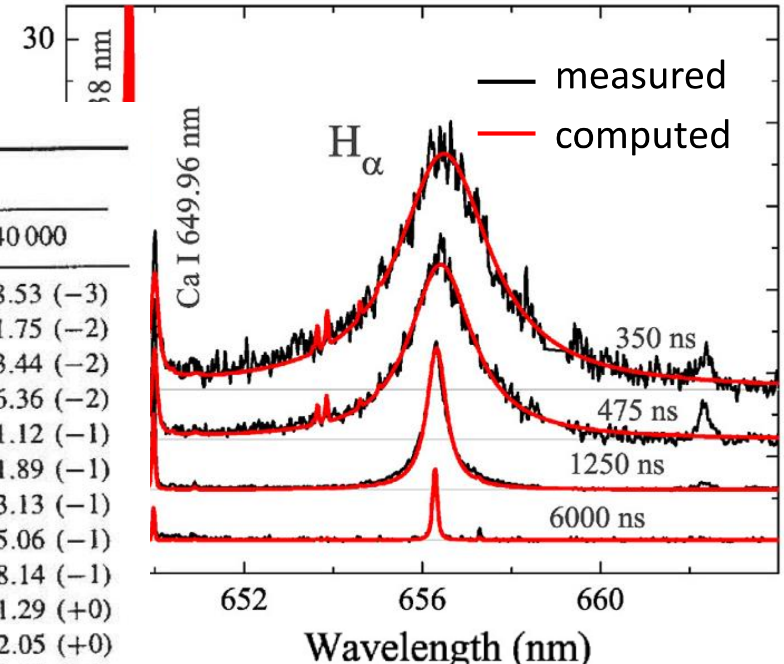

Gigosos and Cardenoso
J. Phys. B 1996

Electron density measurement

using Stark broadening

Stark width $\Delta\lambda_{Stark} = f(n_e, T)$

most simple case

☞ $\Delta\lambda_{Stark} >> \Delta\lambda_{Doppler}, \Delta\lambda_{app}$

example : hydrogen Balmer alpha

$n_e = 1\times10^{17}$ cm^{-3} ⇨ $\Delta\lambda_{Stark} \cong 1$ nm

$T = 1\times10^4$ K ⇨ $\Delta\lambda_{Doppler} \cong 50$ pm

apparatus : $\frac{\lambda}{\Delta\lambda} = 1\times10^4$ ⇨ $\Delta\lambda_{app} = 65$ pm

$$\Rightarrow \Delta\lambda_{Stark} \cong \Delta\lambda_{meas}$$

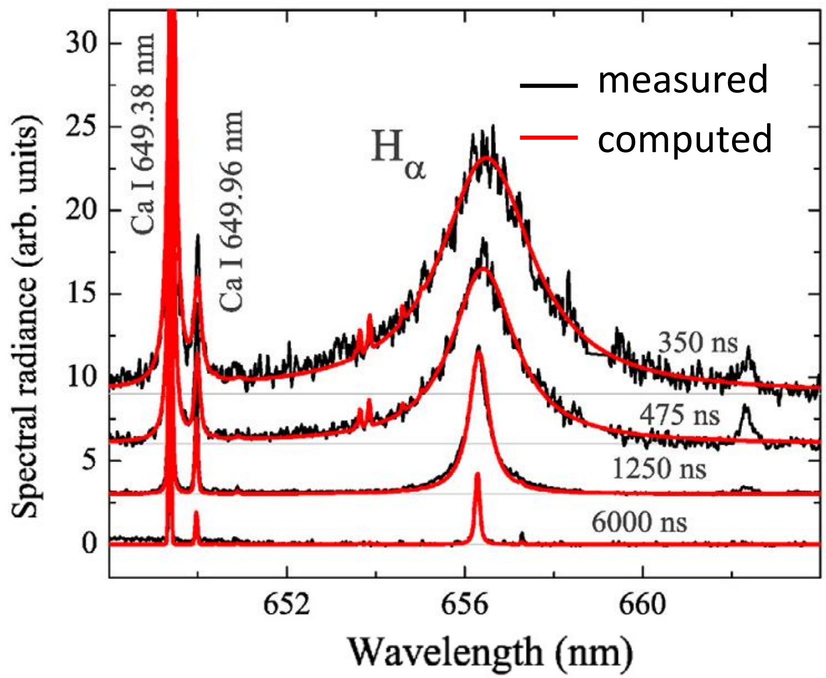

☞ ***n_e* obtained directly from measurement of FWHM**

Electron density measurement

using Stark broadening

Stark width $\Delta\lambda_{Stark} = f(n_e, T)$

for non-hydrogenic lines

☞ **linear dependence**

$$\Delta\lambda_{Stark} \propto n_e$$

neglecting *T*-dependence

$$\Delta\lambda_{Stark} = 2w \frac{n_e}{n_e^{ref}}$$

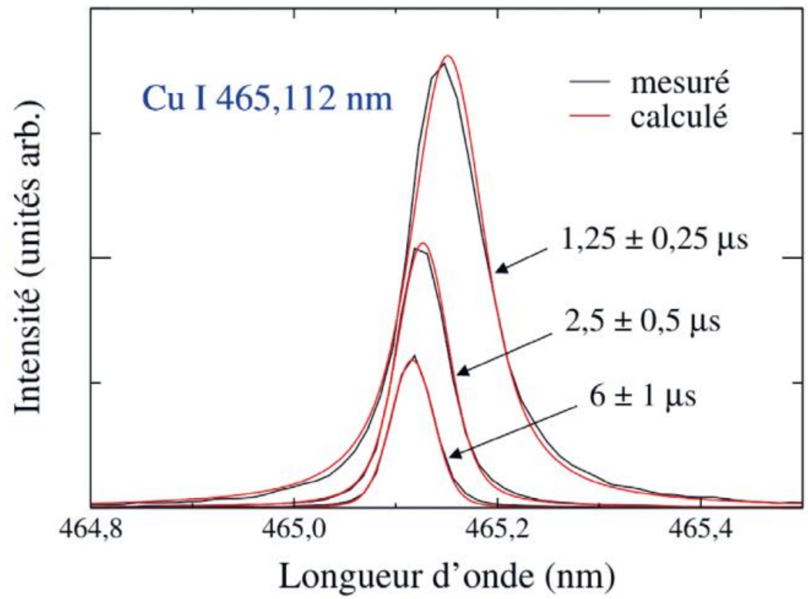

w = Stark broadening parameter

= half-width at half maximum (HWHM) for $n_e = n_e^{ref}$

n_e^{ref} = reference value of n_e for which *w* is given in literature

Electron density measurement

using Stark broadening

Stark width $\Delta\lambda_{Stark} = f(n_e, T)$

for some lines

☞ **analytical expression accounting for *T*-dependence**

$$\Delta\lambda_{Stark} = w\,\frac{n_e}{n_e^{ref}}\left(\frac{T}{T^{ref}}\right)^m$$

Zielinska et al., J. Phys. D (2010)

Fe I 538.33 nm

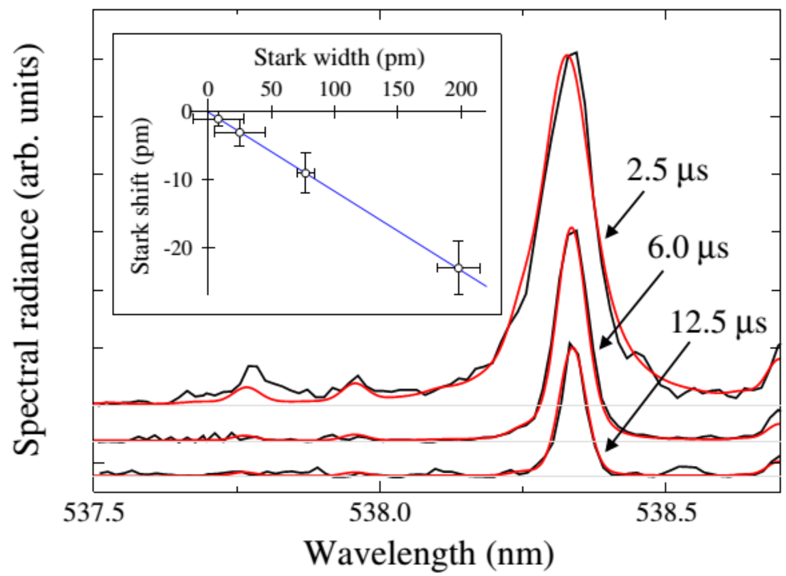

Méthodes de spectroscopie d'émission

pour le diagnostic des plasma produits par ablation laser

Emission from laser-produced plasmas

Spectral line profile

Electron density measurement

Local thermodynamic equilibrium

Temperature measurement

Self-absorption

Non-uniform spatial distribution

Elementary processes

collisional processes :

collisional excitation / desexcitation

$$A^{l} + e^{-}(E) \Leftrightarrow A^{u} + e^{-}(E')$$

electron impact ionization / 3 body recombination

$$A + e^{-}(E) \Leftrightarrow A^{+} + e^{-}(E') + e^{-}(E'')$$

radiative processes :

spontaneous emission / absorption (bound-bound transitions)

$$A^{u} \Leftrightarrow A^{l} + h\nu$$

photoionization / radiative recombination (free-bound transitions)

$$A + h\nu \Leftrightarrow A^{+} + e^{-}(E)$$

bremsstrahlung emission / inverse bremsstrahlung absorption

$$A + e^{-}(E) \Leftrightarrow A + e^{-}(E') \qquad \text{(free-free transitions)}$$

collisional-radiative modeling

☞ **requires rates of all processes**

Local Thermodynamic Equilibrium (LTE)

large plasma density (atmospheric plasmas)

⇨ collisional processes dominate

☞ **simplified description via statistical laws of equilibrium**

velocities :	$f(\upsilon) = 4\pi \left(\frac{m}{2\pi kT} \right)^{3/2} \upsilon^2 \; e^{-m\upsilon^2/2kT}$	*Maxwell*
population densities :	$n_i = n \frac{g_i}{Q} e^{-E_i/kT}$	*Boltzmann*
chemical composition :	$\frac{n_A n_B}{n_{AB}} = \frac{(2\pi \mu kT)^{3/2}}{h^3} \frac{Q_A Q_B}{Q_{AB}} e^{-E_{AB}/kT}$	*Saha*
radiation :	~~$U_\lambda = \frac{2hc^2}{\lambda^5} \frac{1}{e^{hc/\lambda kT} - 1}$~~	*Planck*

g_i = statistical weight of level

E_i = energy of level

Q = partition function

E_{ab} = ionization or dissociation energy

μ = reduced mass = $m_A m_B / (m_A + m_B)$

h = Planck constant

c = speed of light in vacuum

Criteria for validity of LTE

high mobility of electrons (small mass)

⇨ collisional processes dominated by electrons

☞ **validity of LTE depends on electron density**

rates of collisional excitation / desexcitation $\Gamma_{ul}, \Gamma_{lu} >> A_{ul}$

most difficult case ☞ the levels of largest energy gap ΔE_{max}

LTE criterion : $$n_e \geq n_e^* = 6.5 \times 10^{16} \frac{g_u}{g_l} \left(\frac{\Delta E_{max}}{E_H} \right)^3 \sqrt{\frac{kT}{E_H}}$$ *(Drawin, 1970)*

☞ **most elements :** $n_e \geq 10^{16}$ **cm**$^{-3}$

additional criteria :

☞ **transient plasma** $$\frac{T(t+\tau_{rel})-T(t)}{T(t)} << 1 \qquad \frac{n_e(t+\tau_{rel})-n_e(t)}{n_e(t)} << 1$$

☞ **nonuniform plasma** $$\frac{T(x)-T(x+\lambda)}{T(x)} << 1 \qquad \frac{n_e(x)-n_e(x+\lambda)}{n_e(x)} << 1$$

$\lambda = \sqrt{D\,\tau_{rel}}$ = diffusion length during relaxation time

Méthodes de spectroscopie d’émission

pour le diagnostic des plasma produits par ablation laser

Emission from laser-produced plasmas

Spectral line profile

Electron density measurement

Local thermodynamic equilibrium

Temperature measurement

Self-absorption

Non-uniform spatial distribution

Temperature measurement

LTE plasma characterized by unique temperature

Emission coeff. $\varepsilon_{ul} = A_{ul} \dfrac{h\nu}{4\pi} n_u \quad \Rightarrow \quad I_{ul} \propto n_u$ **if optically thin** (no absorption)

Boltzmann $n_u = n \dfrac{g_u}{Q(T)} e^{-E_u/kT}$

Saha $\dfrac{n_i\, n_e}{n_n} = \dfrac{\left(2\pi\,\mu\, kT\right)^{3/2}}{h^3} \dfrac{Q_i\, Q_e}{Q_n} e^{-E_{ion}/kT}$

measurement methods :

- intensity ratio of spectral lines of the same ion
- **Boltzmann plot** (check LTE, spectroscopic data, …)

} *Boltzmann*

- intensity ratio of spectral lines of successive ions (n_e required) *Boltzmann + Saha*
- radiance of a spectral line (requires intensity calibration)
- analysis of continuum (requires apparatus response correction on a large spectral range)

Temperature measurement

requirement ☞ apparatus response correction

$$I_{meas}(\lambda) = R_{app}(\lambda) \times I_{plasma}(\lambda)$$

☞ $R_{app}(\lambda)$ measured using radiation standards

radiation standards:

source	*T* (K)	spectral range (nm)
tungsten filament	≈ 2800	350 … 2400
deuterium arc	≈ 5000	200 … 400

$$\Rightarrow \quad R_{app}(\lambda) = \frac{I_{meas}(\lambda)}{I_{standard}(\lambda)}$$

main difficulty ☞ replace plasma by radiation standard

(use same observation geometry)

Temperature measurement

apparatus response of echelle spectrometer

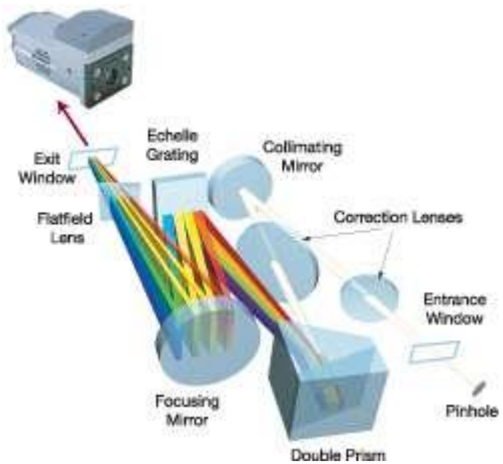

Intensity distribution on CCD detector

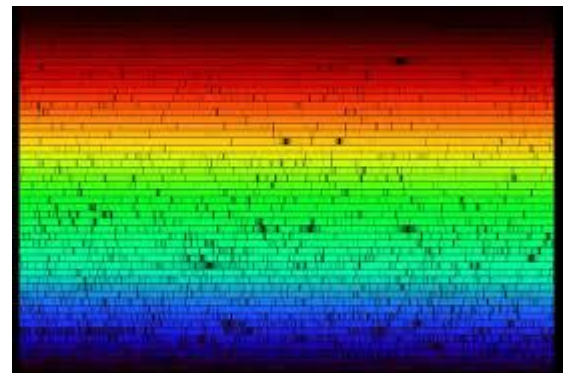

(solar spectrum)

order of diffraction

wavelength

☞ **large band spectrum of high resolution in a single measurement**

☞ echelle spectrometers popular for LIBS analysis of materials

Temperature measurement

apparatus response of echelle spectrometer

example : LIBS apparatus of LP3 laboratory

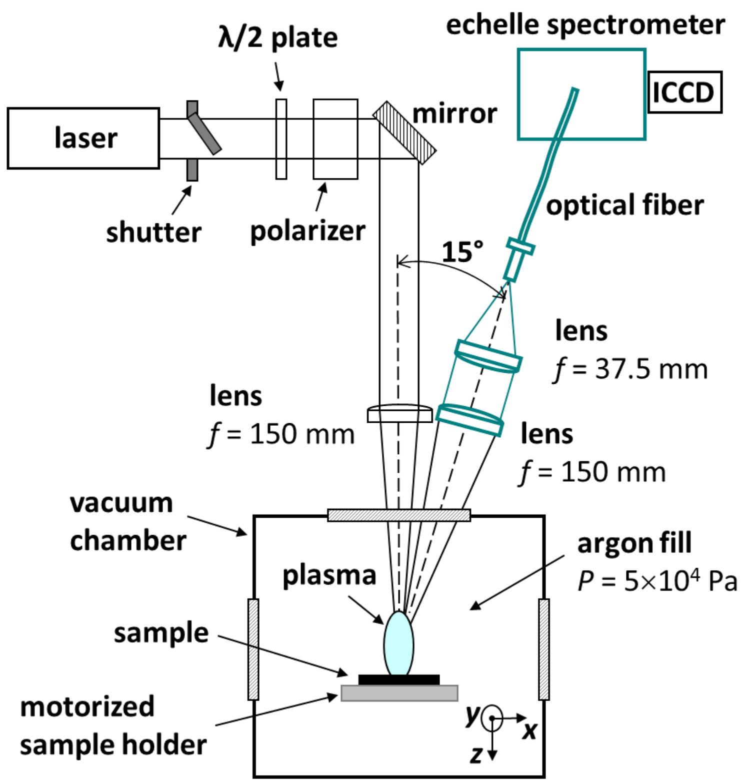

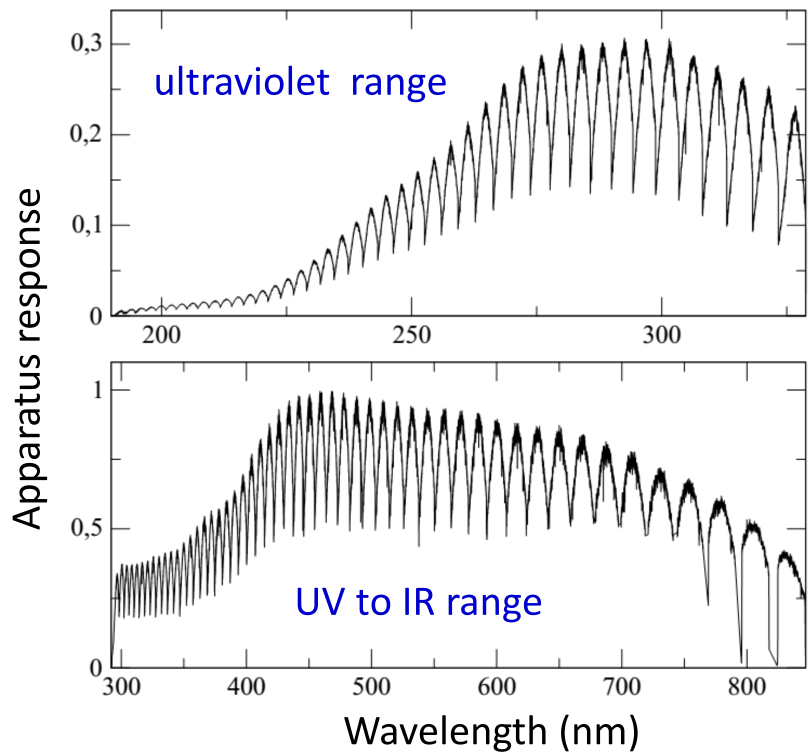

Temperature measurement

LTE plasma characterized by unique temperature

Emission coeff. $\varepsilon_{ul} = A_{ul} \frac{h\nu}{4\pi} n_u \quad \Rightarrow \quad I_{ul} \propto n_u$ **if optically thin** (no absorption)

Boltzmann $n_u = n \frac{g_u}{Q(T)} e^{-E_u/kT}$

Saha $\frac{n_i n_e}{n_n} = \frac{(2\pi \mu kT)^{3/2}}{h^3} \frac{Q_i Q_e}{Q_n} e^{-E_{ion}/kT}$

measurement methods :

- intensity ratio of spectral lines of the same ion
- **Boltzmann plot** (check LTE, spectroscopic data, …)

} *Boltzmann*

- intensity ratio of spectral lines of successive ions (n_e required) *Boltzmann + Saha*
- radiance of a spectral line (requires intensity calibration)
- analysis of continuum (requires apparatus response correction on a large spectral range)

www.nist.gov/pml/atomic-spectra-database

accuracy of transition probabilities

NIST data

copper

most intense lines

Ion	Ritz Wavelength Air (nm)	A_{ki} (s^{-1})	Acc.	E_i (cm^{-1})		E_k (cm^{-1})	Lower Level Conf.	Term	J	Upper Level Conf.	Term	J
Cu I	202.43252	9.8e+06	B	0.000	-	49 383.264	$3d^{10}4s$	^2S	$1/2$	$3d^{10}5p$	$^2P°$	$1/2$
Cu I	202.43383	9.8e+06	B	0.000	-	49 382.945	$3d^{10}4s$	^2S	$1/2$	$3d^{10}5p$	$^2P°$	$3/2$
Cu I	222.57017	4.4e+07	C+	0.000	-	44 915.68	$3d^{10}4s$	^2S	$1/2$	$3d^9(^2D)4s4p(^3P°)$	$^4D°$	$1/2$
Cu I	223.0092			11 202.618	-	56 029.89	$3d^94s^2$	^2D	$5/2$	$3d^9(^2D)4s4p(^1P°)$	$^2F°$	$7/2$
Cu I	224.42670	1.85e+06	C+	0.000	-	44 544.16	$3d^{10}4s$	^2S	$1/2$	$3d^9(^2D)4s4p(^3P°)$	$^4D°$	$3/2$
Cu I	249.21428	2.79e+06	B	0.000	-	40 114.01	$3d^{10}4s$	^2S	$1/2$	$3d^9(^2D)4s4p(^3P°)$	$^4P°$	$3/2$
Cu I	261.83685	3.07e+07		11 202.618	-	49 382.945	$3d^94s^2$	^2D	$5/2$	$3d^{10}5p$	$^2P°$	$3/2$
Cu I	276.63669			13 245.443	-	49 383.264	$3d^94s^2$	^2D	$3/2$	$3d^{10}5p$	$^2P°$	$1/2$
Cu I	276.63913	9.6e+06		13 245.443	-	49 382.945	$3d^94s^2$	^2D	$3/2$	$3d^{10}5p$	$^2P°$	$3/2$
Cu I	296.1164	3.76e+06		11 202.618	-	44 963.26	$3d^94s^2$	^2D	$5/2$	$3d^9(^2D)4s4p(^3P°)$	$^2F°$	$7/2$
Cu I	299.7365			13 245.443	-	46 598.35	$3d^94s^2$	^2D	$3/2$	$3d^9(^2D)4s4p(^3P°)$	$^2D°$	$5/2$
Cu I	301.0835			11 202.618	-	44 406.32	$3d^94s^2$	^2D	$5/2$	$3d^9(^2D)4s4p(^3P°)$	$^4D°$	$5/2$
Cu I	303.6096			13 245.443	-	46 172.89	$3d^94s^2$	^2D	$3/2$	$3d^9(^2D)4s4p(^3P°)$	°	$3/2$
Cu I	306.3410	1.55e+06		13 245.443	-	45 879.32	$3d^94s^2$	^2D	$3/2$	$3d^9(^2D)4s4p(^3P°)$	$^2P°$	$3/2$
Cu I	310.8600			39 018.69	-	71 178.18	$3d^9(^2D)4s4p(^3P°)$	$^4P°$	$5/2$	$3d^94s(^3D)4d$	^4P	$5/2$
Cu I	324.75358	1.395e+08	AA	0.000	-	30 783.697	$3d^{10}4s$	^2S	$1/2$	$3d^{10}4p$	$^2P°$	$3/2$
Cu I	327.39521	1.376e+08	AA	0.000	-	30 535.324	$3d^{10}4s$	^2S	$1/2$	$3d^{10}4p$	$^2P°$	$1/2$
Cu I	327.9809			13 245.443	-	43 726.24	$3d^94s^2$	^2D	$3/2$	$3d^9(^2D)4s4p(^3P°)$	$^2F°$	$5/2$
Cu I	330.7948			40 909.16	-	71 130.68	$3d^9(^2D)4s4p(^3P°)$	$^4F°$	$9/2$	$3d^94s(^3D)4d$	^4G	$11/2$
Cu I	353.0378			13 245.443	-	41 562.93	$3d^94s^2$	^2D	$3/2$	$3d^9(^2D)4s4p(^3P°)$	$^4F°$	$5/2$
Cu I	360.9296			13 245.443	-	40 943.78	$3d^94s^2$	^2D	$3/2$	$3d^9(^2D)4s4p(^3P°)$	$^4P°$	$1/2$
Cu I	406.26378	2.10e+07		30 783.697	-	55 391.297	$3d^{10}4p$	$^2P°$	$3/2$	$3d^{10}5d$	^2D	$5/2$
Cu I	465.1122	3.80e+07		40 909.16	-	62 403.332	$3d^9(^2D)4s4p(^3P°)$	$^4F°$	$9/2$	$3d^94s(^3D)5s$	^4D	$7/2$
Cu I	515.3238	6.0e+07		30 535.324	-	49 935.195	$3d^{10}4p$	$^2P°$	$1/2$	$3d^{10}4d$	^2D	$3/2$
Cu I	521.8202	7.5e+07		30 783.697	-	49 942.051	$3d^{10}4p$	$^2P°$	$3/2$	$3d^{10}4d$	^2D	$5/2$

www.nist.gov/pml/atomic-spectra-database

NIST data
calcium
most intense lines

accuracy
C = 25%
D = 50%

Ion	Ritz Wavelength Air (nm)	A_{ki} (s^{-1})	Acc.	E_i (cm^{-1})		E_k (cm^{-1})	Lower Level Conf., Term, J			Upper Level Conf., Term, J		
Ca II	315.8869	3.1e+08	C	25 191.51	-	56 839.25	$3p^64p$	$^2P°$	$^1/_2$	$3p^64d$	^2D	$^3/_2$
Ca II	317.9331	3.6e+08	C	25 414.40	-	56 858.46	$3p^64p$	$^2P°$	$^3/_2$	$3p^64d$	^2D	$^5/_2$
Ca II	318.1275	5.8e+07	C	25 414.40	-	56 839.25	$3p^64p$	$^2P°$	$^3/_2$	$3p^64d$	^2D	$^3/_2$
Ca II	370.6024	8.8e+07	C	25 191.51	-	52 166.93	$3p^64p$	$^2P°$	$^1/_2$	$3p^65s$	^2S	$^1/_2$
Ca II	373.6902	1.7e+08	C	25 414.40	-	52 166.93	$3p^64p$	$^2P°$	$^3/_2$	$3p^65s$	^2S	$^1/_2$
Ca II	393.3663	1.47e+08	C	0.00	-	25 414.40	$3p^64s$	^2S	$^1/_2$	$3p^64p$	$^2P°$	$^3/_2$
Ca II	396.8469	1.4e+08	C	0.00	-	25 191.51	$3p^64s$	^2S	$^1/_2$	$3p^64p$	$^2P°$	$^1/_2$
Ca II	409.7098	9.9e+06	D	60 533.02	-	84 933.65	$3p^65p$	$^2P°$	$^1/_2$	$3p^67d$	^2D	$^3/_2$
Ca II	410.9815	1.2e+07	D	60 611.28	-	84 936.41	$3p^65p$	$^2P°$	$^3/_2$	$3p^67d$	^2D	$^5/_2$
Ca II	422.0071	8.5e+06	D	60 611.28	-	84 300.89	$3p^65p$	$^2P°$	$^3/_2$	$3p^68s$	^2S	$^1/_2$
Ca I	422.6728	2.18e+08	B+	0.000	-	23 652.304	$3p^64s^2$	^1S	0	$3p^64s4p$	$^1P°$	1
Ca II	500.1479	2.0e+07	D	60 533.02	-	80 521.53	$3p^65p$	$^2P°$	$^1/_2$	$3p^66d$	^2D	$^3/_2$
Ca II	501.9971	2.3e+07	D	60 611.28	-	80 526.16	$3p^65p$	$^2P°$	$^3/_2$	$3p^66d$	^2D	$^5/_2$
Ca II	528.5266	7.8e+06	D	60 533.02	-	79 448.28	$3p^65p$	$^2P°$	$^1/_2$	$3p^67s$	^2S	$^1/_2$
Ca II	530.7224	1.5e+07	D	60 611.28	-	79 448.28	$3p^65p$	$^2P°$	$^3/_2$	$3p^67s$	^2S	$^1/_2$

☞ **accurate A_{ul} values are missing for most elements**

Temperature measurement

Boltzmann plot ☞ check LTE

☞ reduce T-measurement error due to ΔA_{ul}, $\Delta R_{app}(\lambda)$

Emission coeff. $\varepsilon_{ul} = A_{ul}\dfrac{h\nu}{4\pi}n_u \Rightarrow I_{ul} \propto \varepsilon_{ul}$ **if optically thin**

Boltzmann $n_u = n\dfrac{g_u}{Q(T)}e^{-E_u/kT}$ ⇨ $\ln\left(\dfrac{I_{ul}\,\lambda}{A_{ul}\,g_u}\right) = -\dfrac{E_u}{kT} + C^{ste}$

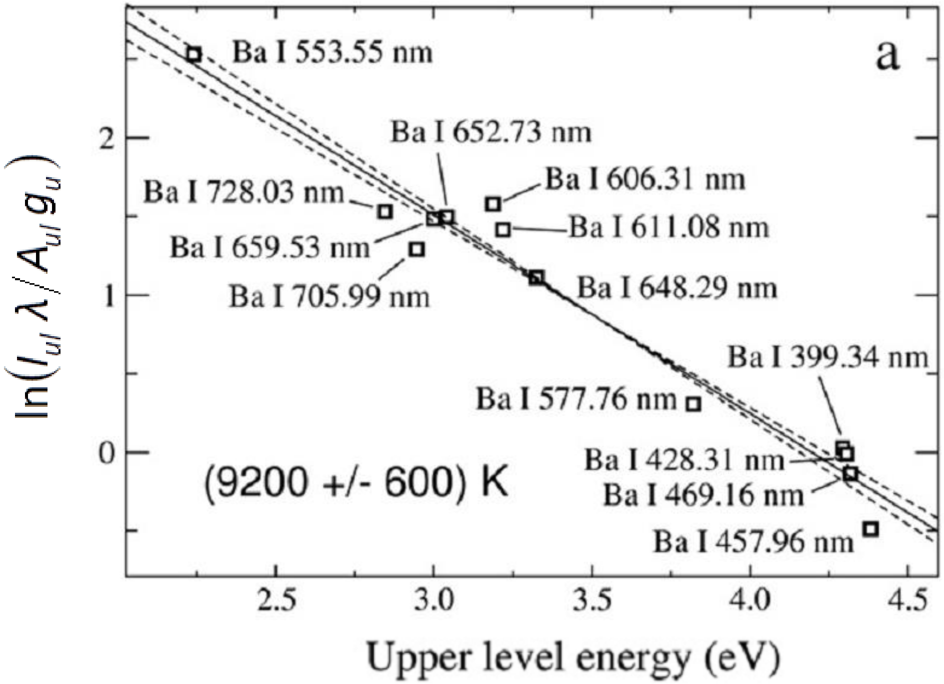

Méthodes de spectroscopie d’émission

pour le diagnostic des plasma produits par ablation laser

Emission from laser-produced plasmas

Spectral line profile

Electron density measurement

Local thermodynamic equilibrium

Temperature measurement

Self-absorption

Non-uniform spatial distribution

Self-absorption

Plasmas in local thermodynamic equilibrium

☞ **high density** (collisional processes dominate)

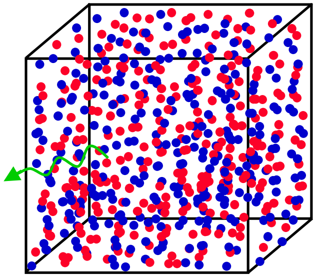

☞ **High density**

⇨ **photons generated by the plasma have non-negligible probability to be re-absorbed**

☞ **self-absorption**

Influence of self-absorption

consider absorption

☞ **solving equation of radiative transfer**

$$n(z)\frac{d}{dz}\left(\frac{I(z)}{n^2(z)}\right) = \varepsilon(z) - \alpha(z)I(z)$$

plasma: $n \cong 1$

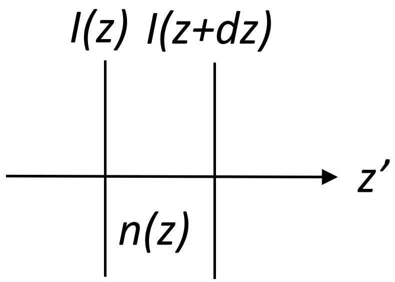

ε = emission coefficient

α = absorption coefficient

n = index of refraction

Influence of self-absorption

consider absorption

☞ **solving equation of radiative transfer**

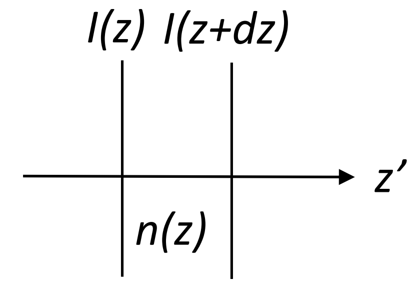

$$n(z)\,\frac{d}{dz}\left(\frac{I(z)}{n^2(z)}\right) = \varepsilon(z) - \cancel{\alpha(z) I(z)}$$

plasma: $n \cong 1$

ε = emission coefficient
α = absorption coefficient
n = index of refraction

☞ **optically thin case** (no absorption**)**

L = plasma size along line of sight

$$\frac{dI(z)}{dz} = \varepsilon(z) \quad \Rightarrow \quad I = \varepsilon L$$

Spectral line: $\varepsilon_{ul} = \int_{\text{profile}} \varepsilon_\lambda \, d\lambda = A_{ul} \frac{h\nu}{4\pi} n_u$

Influence of self-absorption

consider absorption

☞ **solving equation of radiative transfer**

$$n(z)\,\frac{d}{dz}\left(\frac{I(z)}{n^2(z)}\right) = \varepsilon(z) - \alpha(z)I(z)$$

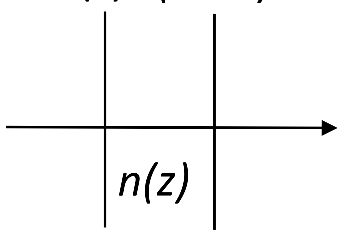

plasma: $n \cong 1$

ε = emission coefficient
α = absorption coefficient
n = index of refraction

☞ **general case** (with absorption)

L = plasma size along line of sight

uniform plasma : $I = I_0\left(1 - e^{-\alpha L}\right)$ with $I_0 = \dfrac{\varepsilon}{\alpha}$

equilibrium ⇨ Kirchhoff's law of thermal radiation $\dfrac{\varepsilon}{\alpha} = B_\lambda^0$

B_λ^0 = blackbody spectral radiance

$$B_\lambda = B_\lambda^0\left(1 - e^{-\tau}\right)$$

optical thickness $\tau = \int_0^L \alpha(z')\,dz' = \alpha L$

Influence of self-absorption

$$B_\lambda = B_\lambda^0(1 - e^{-\tau})$$

weak absorption ☞ **optically thin case** (τ << 1)

$$e^{-\tau} = 1 - \tau + \frac{\tau^2}{2} + \ldots \qquad B_\lambda = B_\lambda^0(1 - e^{-\tau}) \cong B_\lambda^0(1 - 1 + \tau) = B_\lambda^0 \tau = B_\lambda^0 \alpha L$$

Kirchhoff $\frac{\varepsilon}{\alpha} = B_\lambda^0 \quad \Rightarrow \quad B_\lambda \cong \varepsilon L$

strong absorption ☞ **optically thick case** (τ >> 1)

$$\Rightarrow B_\lambda \cong B_\lambda^0$$

⇨ **strong lines saturate at blackbody radiance**

Simulation of emission spectrum

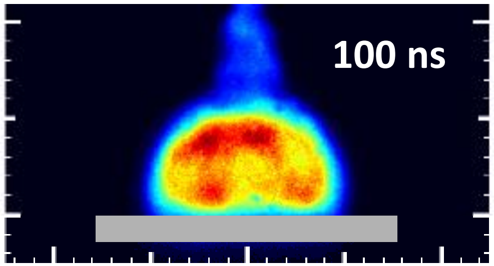

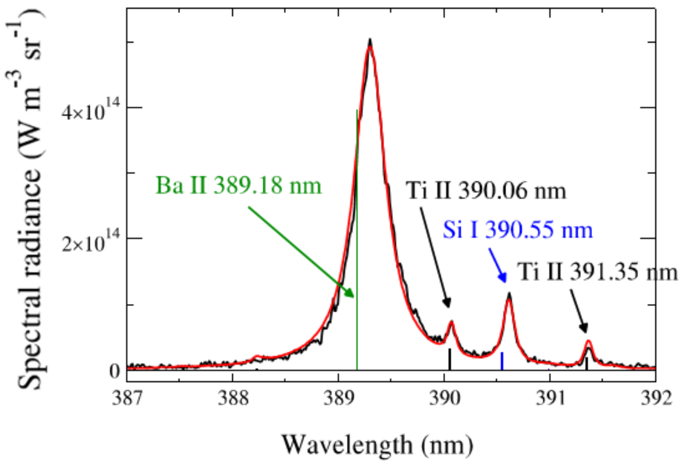

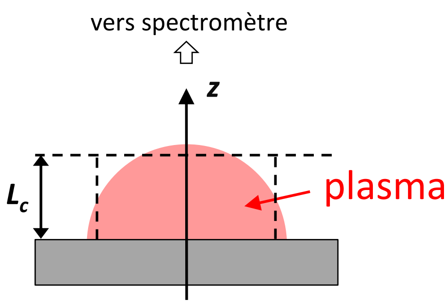

$\Rightarrow$ Spectral radiance $B_\lambda = B_\lambda^0 (1 - e^{-\tau})$

$$\alpha_{line}(\lambda) = \pi r_0 \lambda^2 f_{lu} n_l P(\lambda_0, \lambda)\left(1 - e^{-hc/\lambda kT}\right)$$

Doppler and Stark broadening

B_λ^0 = blackbody spectral radiance

τ = optical thickness = $\int \alpha(\lambda, z) dz = \alpha(\lambda) L$

α = absorption coefficient = $\sum_i \alpha_{line}^{(i)} + \alpha_{ion} + \alpha_{IB}$

L = plasma diameter along line of sight

☞ **fast calculation**

Influence of self-absorption

on spectral line intensity

$\Rightarrow$ Spectral radiance $B_\lambda = U_\lambda\left(1 - e^{-\tau}\right)$

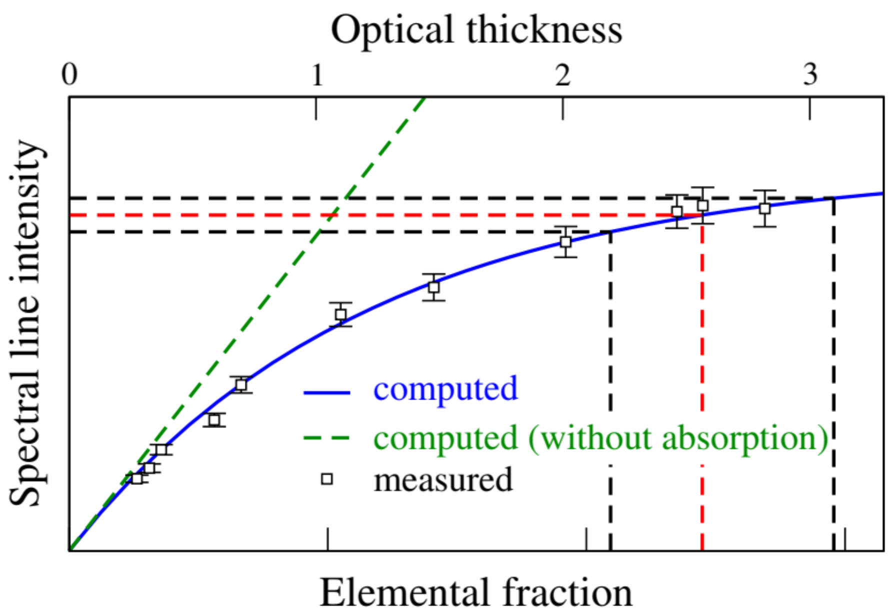

☞ **strong self-absorption** (τ >> 1) $\Rightarrow$ $B_\lambda = U_\lambda$

⇨ strong lines saturate at blackbody radiance

Influence of self-absorption

on spectral line shape

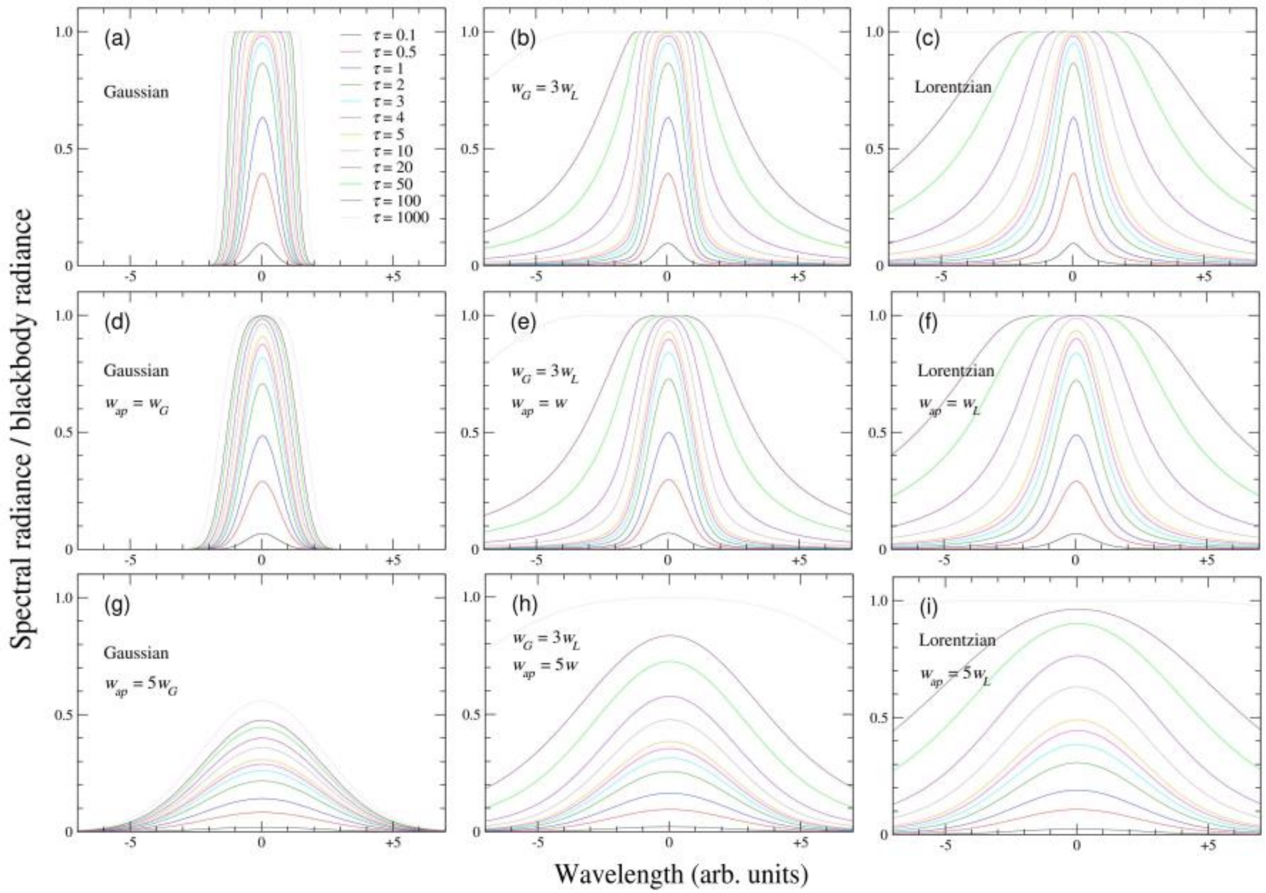

☞ **Intensity lowering due self-absorption to depends on line shape**

Influence of self-absorption

on spectral line shape

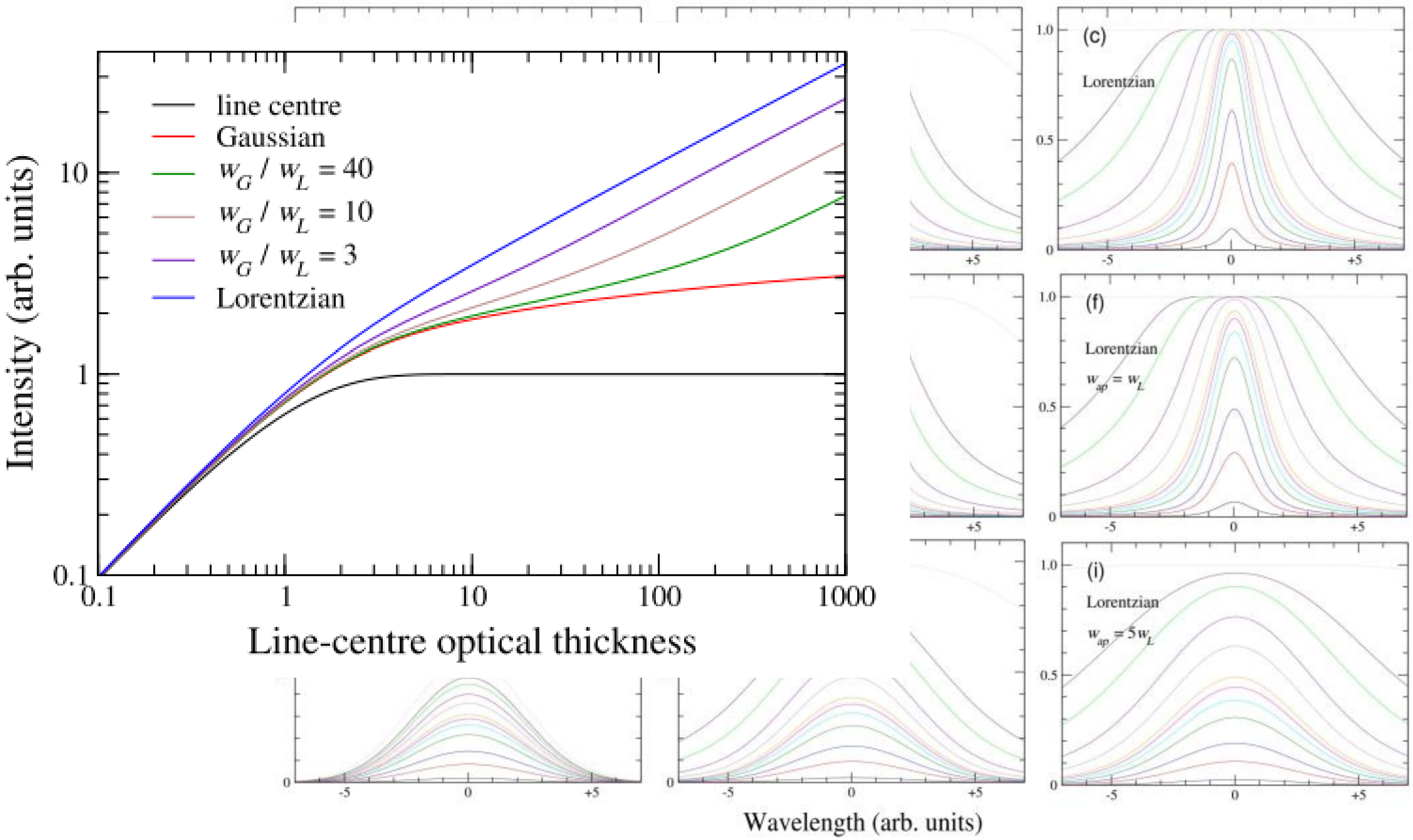

☞ **Intensity lowering due self-absorption to depends on line shape**

Influence of self-absorption

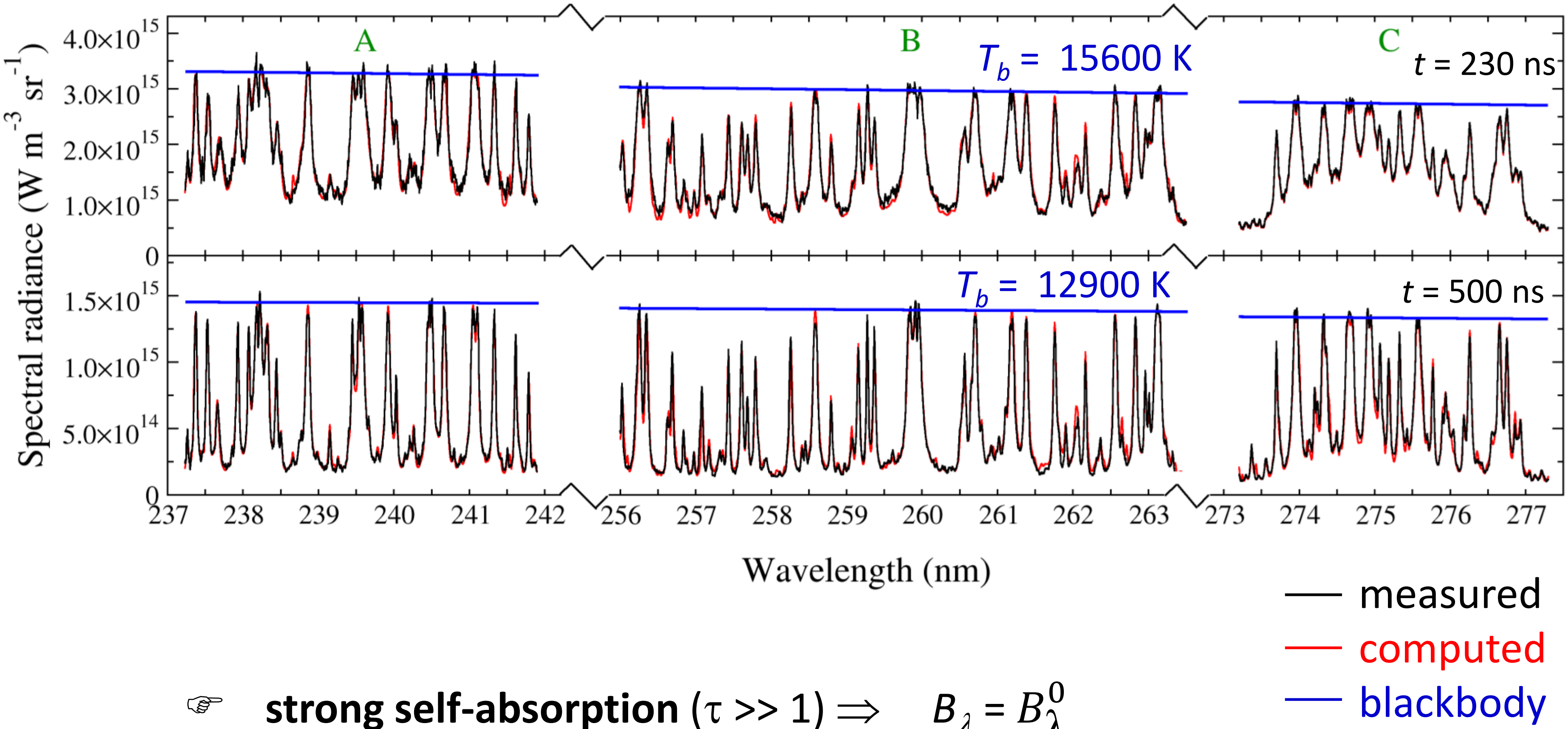

☞ **strong self-absorption** ($\tau >> 1$) $\Rightarrow$ $B_\lambda = B^0_\lambda$

⇨ **strong lines saturate at blackbody radiance**

Méthodes de spectroscopie d'émission

pour le diagnostic des plasma produits par ablation laser

Emission from laser-produced plasmas

Spectral line profile

Electron density measurement

Local thermodynamic equilibrium

Temperature measurement

Self-absorption

Non-uniform spatial distribution

Non-uniform spatial distribution

Profil spectral d'une raie à fort déplacement Stark

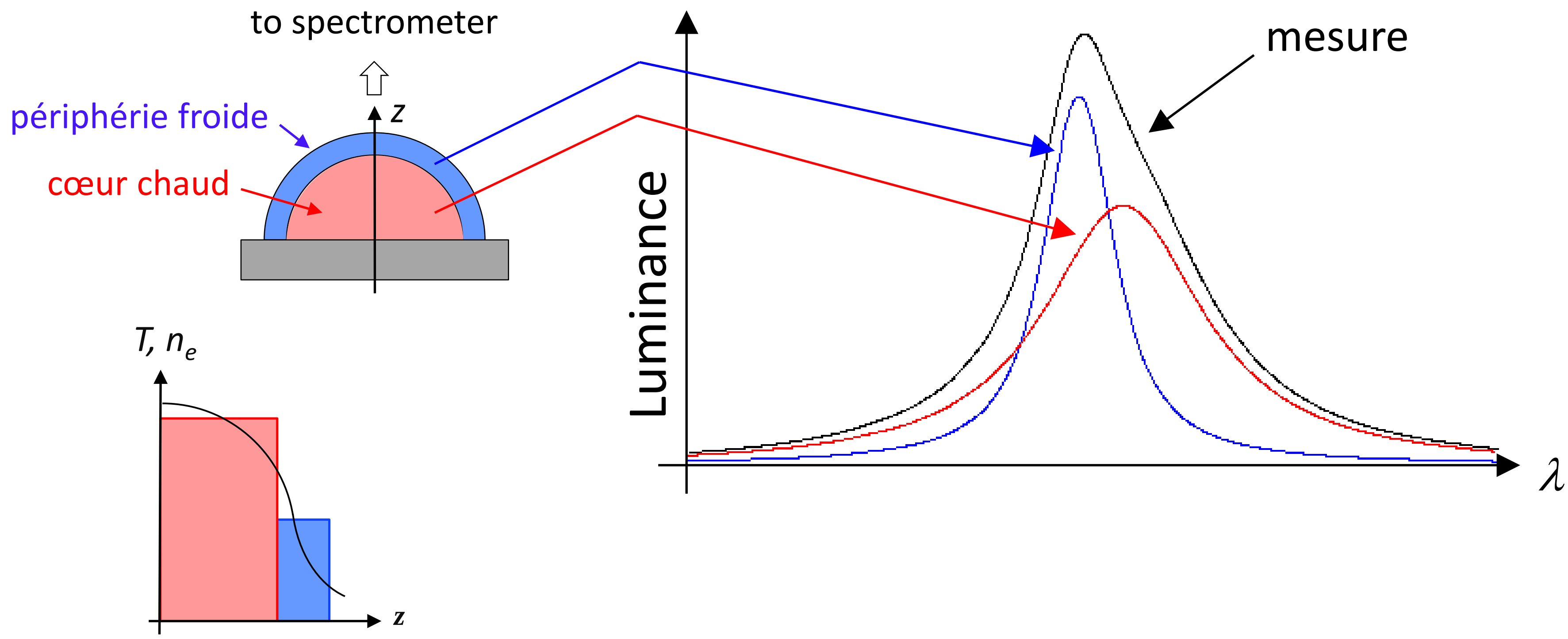

plasma non-uniforme ⇨ profile asymétrique

Non-uniform spatial distribution

Profil spectral d'une raie à fort déplacement Stark

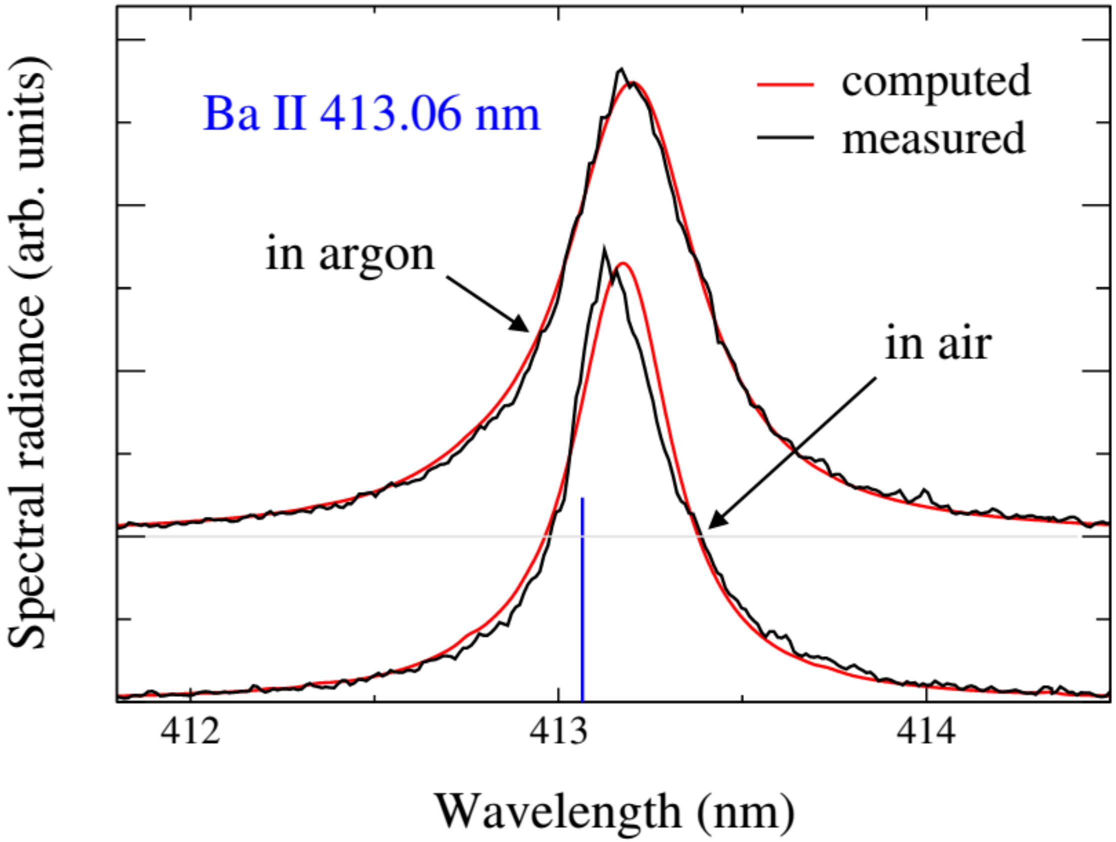

verre N-BaK4

E_{las} = 6 mJ, λ = 266 nm, τ = 5 ns

sous air

☞ **plasma non-uniforme**

sous argon

☞ **plasma uniforme**

Non-uniform spatial distribution

Transition fortement auto-absorbée

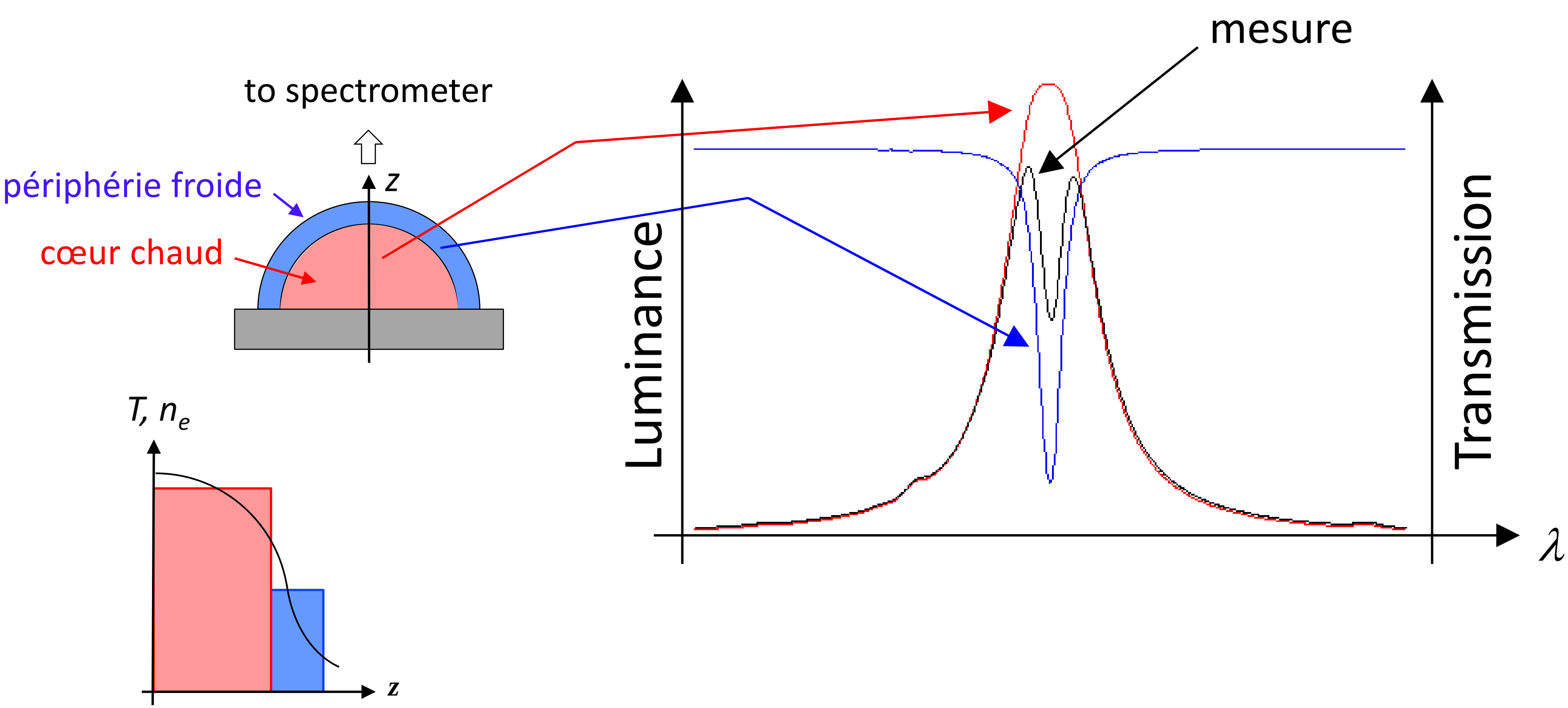

périphérie froide ⇨ creux d'absorption

Non-uniform spatial distribution

Transition fortement auto-absorbée

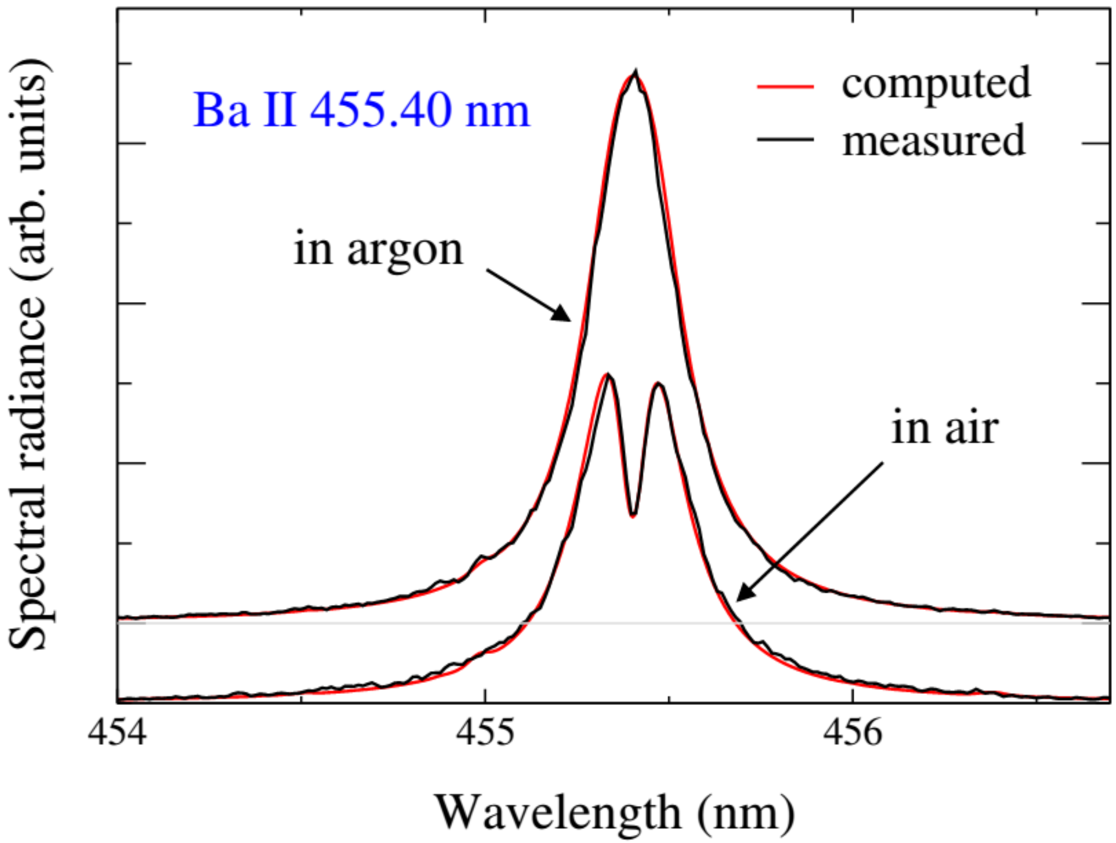

verre N-BaK4

E_{las} = 6 mJ, λ = 266 nm, τ = 5 ns

sous air

☞ **plasma non-uniforme**

sous argon

☞ **plasma uniforme**

Non-uniform spatial distribution

simplified description

☞ **dividing plasma into two zones**

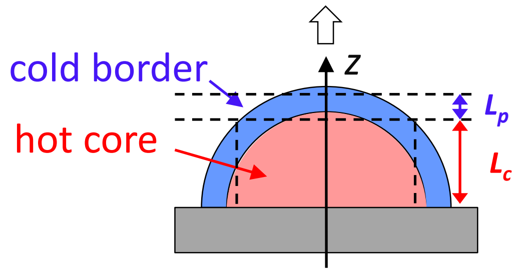

spectral radiance :

$$B = U_C\left(1-e^{-\alpha_C L_C}\right)e^{-\alpha_P L_P} + U_P\left(1-e^{-\alpha_P L_P}\right)$$

absorption coefficient :

$$\alpha(\lambda,T) = \pi\, r_0\, \lambda^2\, f_{lu}\, n_l\, P(\lambda_0,\lambda)\left(1-e^{-hc/\lambda kT}\right)$$

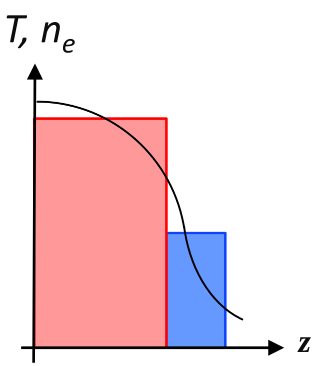

U = blackbody spectral radiance

r_0 = classical electron radius

f_{lu} = absorption oscillator strength

n_l = lower level number density

P = normalized line profile

Non-uniform spatial distribution

Ablation of Al in ambient air ☞ molecular emission from cold border

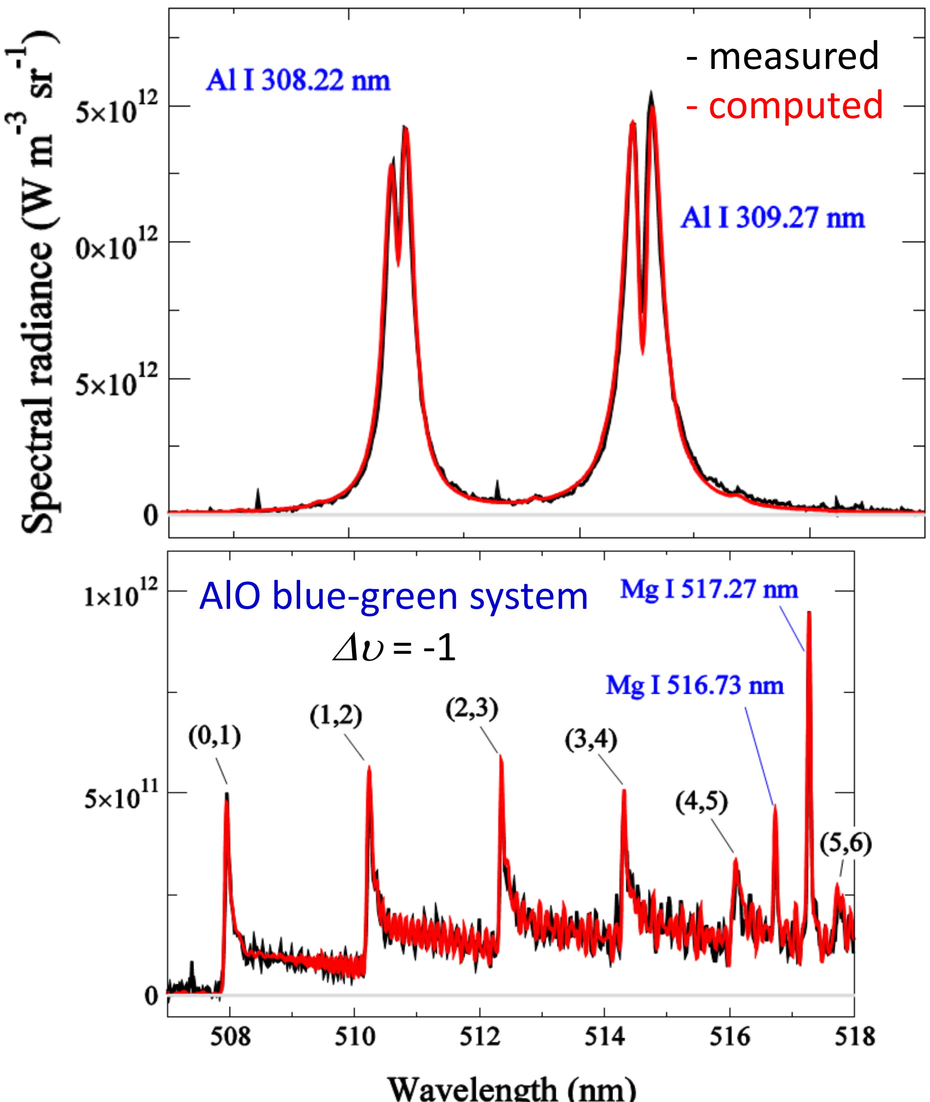

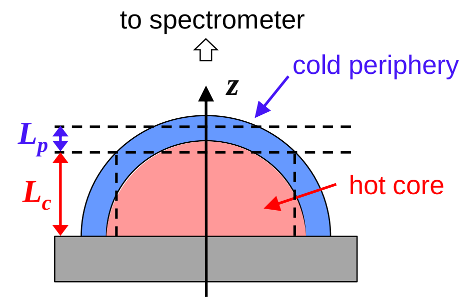

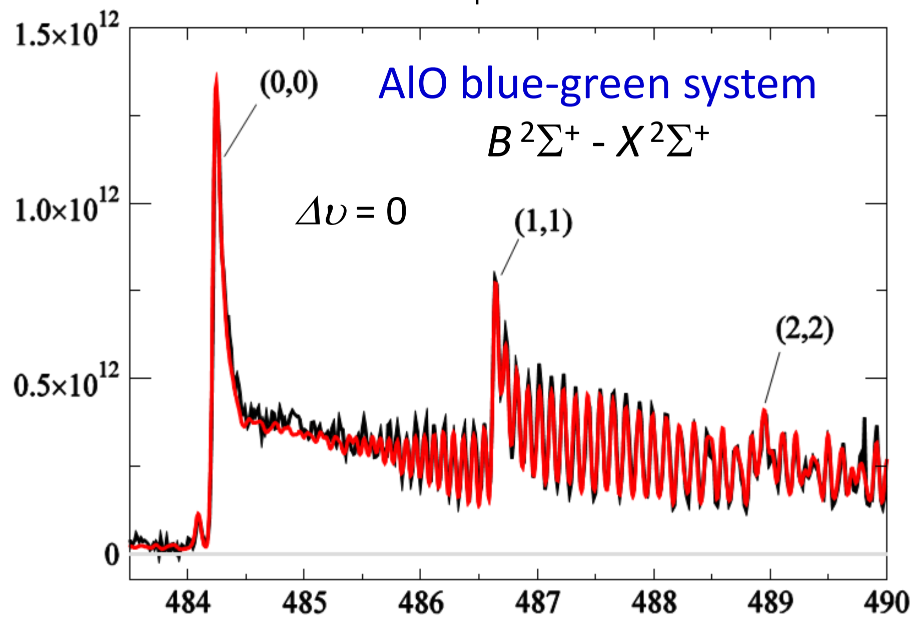

Hermann et al., Phys. Rev. E 2015